
Task-Aware Network Coding Over Butterfly Network

Jiangnan Cheng¹ Sandeep Chinchali² Ao Tang¹

Abstract

Network coding allows distributed information sources such as sensors to efficiently compress and transmit data to distributed receivers across a bandwidth-limited network. Classical network coding is largely task-agnostic – the coding schemes mainly aim to faithfully reconstruct data at the receivers, regardless of what ultimate task the received data is used for. In this paper, we analyze a new *task-driven* network coding problem, where distributed receivers pass transmitted data through machine learning (ML) tasks, which provides an opportunity to improve efficiency by transmitting salient task-relevant data representations. Specifically, we formulate a *task-aware* network coding problem over a butterfly network in real-coordinate space, where lossy analog compression through principal component analysis (PCA) can be applied. A lower bound for the total loss function for the formulated problem is given, and necessary and sufficient conditions for achieving this lower bound are also provided. We introduce ML algorithms to solve the problem in the general case, and our evaluation demonstrates the effectiveness of task-aware network coding.

1. Introduction

Distributed sensors measure rich sensory data which potentially are consumed by multiple distributed data receivers. On the other hand, network bandwidths remain limited and expensive, especially for wireless networks. For example, low Earth orbit satellites collect high-resolution Earth imagery, whose size goes up to few terabytes per day and is sent to geographically distributed ground stations, while in the best case one ground station can only download 80 GB from one satellite in a single pass (Vasisht et al., 2021).

¹School of Electrical and Computer Engineering, Cornell University, Ithaca, NY ²Department of Electrical and Computer Engineering, The University of Texas at Austin, Austin, TX. Correspondence to: Jiangnan Cheng <jc3377@cornell.edu>, Sandeep Chinchali <sandeepc@utexas.edu>, Ao Tang <atang@cornell.edu>.

Therefore, one is motivated to make efficient use of the existing network bandwidths for *distributed* data sources and receivers.

Network coding (Ahlsweede et al., 2000) is an important technology which aims at maximizing the network throughput for multi-source multicasting with limited network bandwidths. Classical network coding literatures (Li et al., 2003; Koetter & Médard, 2003; Dougherty et al., 2005; Jaggi et al., 2005; Ho et al., 2006; Chen et al., 2008) consider a pure network information flow problem from the information-theoretic view, where the demands for all the data receivers, either homogeneous or heterogeneous, are specified and the objective is to satisfy each demand with a rate (i.e., mutual information between the demand and the received data) as high as possible. However, in reality each data receiver may apply the received data to a different task, such as inference, perception and control, where different lossy data representations, even with the same rate, can produce totally different task losses. Hence it is highly prominent to transmit *salient* task-relevant data representations to distributed receivers that satisfy the network topology and bandwidth constraints, rather than representations with the highest rate.

Therefore, we formulate a concrete task-aware network coding problem in this paper, as shown in Fig. 1(b). Our problem focuses on *task-aware* linear network coding over butterfly network. Moreover, the domain of our problem is multi-dimensional real-coordinate space \mathbb{R}^n rather than finite field $\text{GF}(\cdot)$ as in classical network coding literatures, which enables us to consider lossy analog compression (similar to Wu & Verdú (2010)) through principal component analysis (PCA) (Dunteman, 1989) rather than information-theoretic discrete compression.

Related work. Our work is broadly related to network coding and task-aware representation learning. First, beyond those classical network coding literatures, the two closest works to ours are Liu et al. (2020) and Whang et al. (2021), where *data-driven* approach is adopted in the general network coding and distributed source coding settings respectively, to determine a coding scheme that minimizes *task-agnostic* reconstruction loss. In stark contrast, we aim at finding a linear network coding scheme that minimizes an overall *task-aware* loss which incorporates heterogeneous task objectives of different receivers,

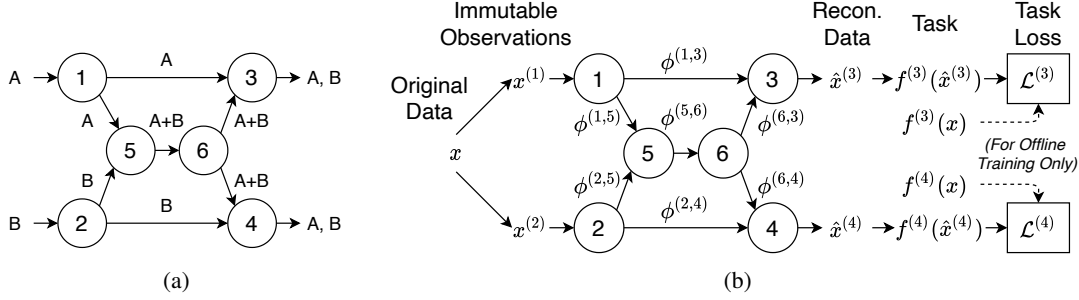


Figure 1. Network coding over butterfly network. Left (classical setting): Task-agnostic network coding in finite field. Node 3 can decode B through $A+(A+B)$ where ‘+’ represents exclusive or logic. Node 4 can decode A similarly. Right (our setting): Task-aware network coding in real-coordinate space. Salient task-relevant data representations are transmitted to make efficient use of network bandwidths.

and we show that in some cases such linear coding scheme can even be determined analytically. Second, our work is also related to network functional compression problem (Doshi et al., 2010; Feizi & Médard, 2014; Shannon, 1956; Slepian & Wolf, 1973; Ahlswede & Korner, 1975; Wyner & Ziv, 1976; Korner & Marton, 1979), where a general function with distributed inputs over finite space is compressed. There’s a similar task-aware loss function in our work, yet it corresponds to machine learning tasks over multi-dimensional real-coordinate space. Lastly, there have been a variety of works (Blau & Michaeli, 2019; Nakanoya et al., 2021; Dubois et al., 2021; Zhang et al., 2021; Cheng et al., 2021) focusing on task-aware data compression for inference, perception and control tasks under a single-source single-destination setting which is similar to Shannon’s rate-distortion theory (Shannon et al., 1959), while in contrast we consider task-aware data compression in a *distributed* setting.

Contributions. In light of prior work, our contributions are three-fold as follows. First, we formulate a task-aware network coding problem over butterfly network in real-coordinate space where lossy analog compression through PCA can be applied (Sec. 3). Second, we give a lower bound for the formulated problem, and provide necessary condition and sufficient conditions for achieving such lower bound (Sec. 4). Third, we adopt standard machine learning algorithm to solve the formulated problem in the general case (Sec. 5), and validate the effectiveness of task-aware network coding in our evaluation (Sec. 6).

2. Preliminaries

Network Coding with a Classical Example. Network coding (Ahlswede et al., 2000) is a technique to increase the network throughput for multi-source multicasting under limited network bandwidths. The key idea of network coding is to allow each node within the network to encode and decode data rather than simply routing it.

A classical example over butterfly network in finite field $\text{GF}(2)$, as shown in Fig. 1(a), is widely used to illustrate the benefit of network coding. The butterfly network can be represented by a directed graph $\mathcal{G} = (\mathcal{V}, \mathcal{E})$. Here $\mathcal{V} = \{1, 2, \dots, 6\}$ is the set of nodes, and $\mathcal{E} = \{(1, 3), (1, 5), (2, 4), (2, 5), (5, 6), (6, 3), (6, 4)\}$ is the set of edges, where (i, j) represents an edge with source node i and destination node j . Suppose each edge in \mathcal{E} can only carry a single bit, and node 1 and 2 each have a single bit of information, denoted by A and B respectively, which are supposed to be multicast to both node 3 and 4. In this case, network coding, as illustrated in Fig. 1(a), makes such multicasting possible while routing cannot. The key idea is to encode A and B as $A+B$ at node 5, where ‘+’ here represents exclusive or logic. Node 3 is able to decode B through $A+(A+B)$, and node 4 can decode A similarly.

Task-aware PCA. PCA is a widely-used dimensionality-reduction technique, and has been used in Nakanoya et al. (2021); Cheng et al. (2021), etc., for task-aware data compression under a single-source single-destination setting.

Suppose we have an n -dimensional random vector $x \in \mathbb{R}^n$, with mean $\mathbb{E}_x[x] = \mathbf{0}$ and positive definite covariance matrix $\Psi = \mathbb{E}_x[xx^T]$ (i.e., $\text{rank}(\Psi) = n$). Consider the following task-aware data compression problem:

$$\min_{D, E} \mathcal{L} = \mathbb{E}_x[\|f(x) - f(\hat{x})\|_2^2] \quad (1)$$

$$\text{s.t. } \hat{x} = DEx, D \in \mathbb{R}^{n \times Z}, E \in \mathbb{R}^{Z \times n} \quad (2)$$

where \hat{x} is the reconstructed vector through a bottlenecked channel which only transmits a low-dimensional vector in \mathbb{R}^Z such that $Z \leq n$, and $E \in \mathbb{R}^{Z \times n}$ and $D \in \mathbb{R}^{n \times Z}$ are the corresponding encoding and decoding matrices respectively. Loss function \mathcal{L} is associated with a task function $f(\cdot) \in \mathbb{R}^m$ and captures the mean-squared error between $f(x)$ and $f(\hat{x})$. In this paper we consider linear task function $f(x) = Kx$, where $K \in \mathbb{R}^{m \times n}$ is called task matrix.

According to PCA, the optimal task loss \mathcal{L}^* can be determined as follows. Suppose the Cholesky decompo-

sition of Ψ is $\Psi = LL^\top$ where $L \in \mathbb{R}^{n \times n}$ is a lower triangular matrix with positive diagonal entries, and the eigen-values in descending order and the corresponding normalized eigen-vectors of Gram matrix $S = L^\top K^\top KL$ are $\mu_1, \mu_2, \dots, \mu_n$ and u_1, u_2, \dots, u_n respectively. Then we have $\mathcal{L}^* = \sum_{i=Z+1}^n \mu_i$, and if the eigen-gap $\mu_Z - \mu_{Z+1} > 0$ (define $\mu_{n+1} = 0$), we must have $\text{col}(E^\top) = \text{span}(\{L^{-\top}u_1, L^{-\top}u_2, \dots, L^{-\top}u_Z\})$ to achieve minimum task loss, where $\text{col}(\cdot)$ denotes the column space of a matrix and $\text{span}(\cdot)$ denotes the linear span of a set of vectors. See Sec. A.1 for a detailed derivation.

3. Problem Formulation

We now formulate a task-aware network coding problem over butterfly network, as shown in Fig. 1(b). The key differences between our formulation and the classical example in Fig. 1(a) are: 1) our formulation has a heterogeneous task objective for each receiver while the classical example does not; 2) the domain of code is multi-dimensional real-coordinate space in our formulation rather than finite space as in the classical example, and hence PCA can be applied.

Data. The original data is a random vector $x = [x_1, x_2, \dots, x_n]^\top \in \mathbb{R}^n$, where $x_i \in \mathbb{R}$ is a random variable, $\forall i \in \{1, 2, \dots, n\}$. Without loss of generality, we assume $\mathbb{E}_x[x] = \mathbf{0}$, or else we replace x by $x - \mathbb{E}_x[x]$. We also let $\Psi = \mathbb{E}_x[xx^\top]$ be the covariance matrix of x .

Data observations. Node 1 and 2 have immutable partial observations of x , denoted by $x^{(1)} \in \mathbb{R}^a$ and $x^{(2)} \in \mathbb{R}^b$, respectively. Here observations $x^{(1)}$ and $x^{(2)}$ are composed of a and b different dimensions of x , respectively; and each x_i exists in *at least* one of the two observations. Therefore, we have $\max\{a, b\} \leq n \leq a + b$. Without loss of generality, we let $x^{(1)} = [x_1, x_2, \dots, x_a]^\top$ and $x^{(2)} = [x_{n-b+1}, x_{n-b+2}, \dots, x_n]^\top$. That is, $x_{1:n-b}$ and $x_{a+1:n}$ are node 1's and node 2's exclusive observations respectively, and $x_{n-b+1:a}$ are their mutual observations.

Data transmission. We assume all the edges have the same capacity Z , which represents the number of dimensions in real-coordinate space here. And $\forall (i, j) \in \mathcal{E}$, we use $\phi^{(i,j)} \in \mathbb{R}^Z$ to denote the random vector that transmits over the edge (i, j) . Notice that for each edge $(i, j) \in \mathcal{E}' = \{(1, 3), (1, 5), (2, 4), (2, 5), (5, 6)\}$, the overall number of input dimensions for node i can be larger than Z , so we use linear mappings to transform the input signal to a low-dimensional signal in \mathbb{R}^Z :

$$\phi^{(1,3)} = E^{(1,3)}x^{(1)}, \phi^{(1,5)} = E^{(1,5)}x^{(1)}, \quad (3)$$

$$\phi^{(2,4)} = E^{(2,4)}x^{(2)}, \phi^{(2,5)} = E^{(2,5)}x^{(2)}, \quad (4)$$

$$\phi^{(5,6)} = E^{(5,6)} \begin{bmatrix} \phi^{(1,5)} \\ \phi^{(2,5)} \end{bmatrix}, \quad (5)$$

where $E^{(1,3)}, E^{(1,5)} \in \mathbb{R}^{Z \times a}$, $E^{(2,4)}, E^{(2,5)} \in \mathbb{R}^{Z \times b}$, and

$E^{(5,6)} \in \mathbb{R}^{Z \times 2Z}$ are encoding matrices. Node 6 simply multicasts the data received from node 5 to node 3 and node 4, i.e., $\phi^{(6,3)} = \phi^{(6,4)} = \phi^{(5,6)}$.

Data reconstructions. Node 3 and 4 aim to reconstruct the original data x , through the aggregated inputs they received from their respective input edges. The corresponding decoder functions are as follows:

$$\hat{x}^{(3)} = D^{(3)} \begin{bmatrix} \phi^{(1,3)} \\ \phi^{(6,3)} \end{bmatrix}, \hat{x}^{(4)} = D^{(4)} \begin{bmatrix} \phi^{(2,4)} \\ \phi^{(6,4)} \end{bmatrix}, \quad (6)$$

where $D^{(3)}, D^{(4)} \in \mathbb{R}^{n \times 2Z}$ are decoding matrices for node 3 and node 4 respectively, and $\hat{x}^{(3)}$ and $\hat{x}^{(4)}$ are the reconstructed data at node 3 and node 4 respectively.

Task objectives. Node i ($\forall i \in \{3, 4\}$) uses the reconstructed data $\hat{x}^{(i)}$ as the input for a task with the following loss function:

$$\mathcal{L}^{(i)} = \mathbb{E}_x[\|f^{(i)}(x) - f^{(i)}(\hat{x}^{(i)})\|_2^2], \quad \forall i \in \{3, 4\} \quad (7)$$

where $f^{(i)}(x) = K^{(i)}x$ with task matrix $K^{(i)} \in \mathbb{R}^{m_i \times n}$. Our overall task loss $\mathcal{L}_{\text{total}}$ is the sum of $\mathcal{L}^{(3)}$ and $\mathcal{L}^{(4)}$:

$$\mathcal{L}_{\text{total}} = \mathcal{L}^{(3)} + \mathcal{L}^{(4)}. \quad (8)$$

Task-aware network coding problem. The problem can be written as an optimization problem:

$$\min_{E^{(i,j)}, D^{(i)}} \mathcal{L}_{\text{total}}, \quad \text{s.t. Eq.(3) - (6)} \quad (9)$$

where we find the optimal encoder and decoder parameters to minimize the overall task loss $\mathcal{L}_{\text{total}}$. And we denote the problem by *TaskAwareCoding*($n, \Psi, a, b, Z, K^{(3)}, K^{(4)}$) for given parameters $n, \Psi, a, b, Z, K^{(3)}, K^{(4)}$.

4. Analysis

In this section, we give detailed analysis towards the task-aware network coding problem. In Sec. 4.1 we provide a lower bound $\mathcal{L}_{\text{total,lb}}$ which may not be always achievable, and in Sec. 4.2 and Sec. 4.3 we discuss necessary condition and sufficient conditions for $\mathcal{L}_{\text{total}}^* = \mathcal{L}_{\text{total,lb}}$, respectively.

4.1. Lower bound $\mathcal{L}_{\text{total,lb}}$

We first show in the following Theorem 4.1 that making the assumption of $\text{rank}(\Psi) = n$ doesn't make the task-aware network coding problem lose generality. The proof is given in Sec. A.2 due to space limit.

Theorem 4.1. *For any $n, \Psi, a, b, Z, K^{(3)}, K^{(4)}$, we can transform *TaskAwareCoding*($n, \Psi, a, b, Z, K^{(3)}, K^{(4)}$) to *TaskAwareCoding*($\tilde{n}, \tilde{\Psi}, \tilde{a}, \tilde{b}, Z, \tilde{K}^{(3)}, \tilde{K}^{(4)}$) where $\tilde{n}, \tilde{\Psi}, \tilde{a}, \tilde{b}, Z, \tilde{K}^{(3)}, \tilde{K}^{(4)}$ is a set of parameters with $\text{rank}(\tilde{\Psi}) = \tilde{n}$, such that their optimal overall task losses are equal, and an optimal solution for one problem can be transformed to the optimal solution for another linearly.*

Therefore, in the rest of the analysis, we simply assume $\text{rank}(\Psi) = n$, and we let the Cholesky decomposition of Ψ be LL^\top , where $L \in \mathbb{R}^{n \times n}$. Moreover, notice that $\phi^{(i,j)}$ is a linear transformation from x and hence is also a linear transformation from $L^{-1}x$. Therefore, for the convenience of the following analysis we let $\phi^{(i,j)} = \Phi^{(i,j)\top} L^{-1}x$ where $\Phi^{(i,j)} \in \mathbb{R}^{n \times Z}$ is a transformation matrix. Furthermore, we assume $Z \leq n$, or else the network is not bottlenecked and the optimal solution is trivial.

For task matrix $K^{(i)}, \forall i \in \{3, 4\}$, we define Gram matrix $S^{(i)} = L^\top K^{(i)\top} K^{(i)} L \in \mathbb{R}^{n \times n}$. Moreover, let the eigen-values in descending order and the corresponding normalized eigen-vectors of $S^{(i)}$ be $\mu_1^{(i)}, \mu_2^{(i)}, \dots, \mu_n^{(i)}$ and $u_1^{(i)}, u_2^{(i)}, \dots, u_n^{(i)}$, respectively. Since node 3 receives $[\phi^{(1,3)\top}, \phi^{(5,6)\top}]^\top$ which has $2Z$ dimensions, according to PCA (as in Sec. 2), we have $\mathcal{L}^{(3)} \geq \sum_{j=2Z+1}^n \mu_j^{(3)}$. Similarly, $\mathcal{L}^{(4)} \geq \sum_{j=2Z+1}^n \mu_j^{(4)}$. Therefore, $\mathcal{L}_{\text{total}} \geq \mathcal{L}_{\text{total,lb}}$ where $\mathcal{L}_{\text{total,lb}} = \sum_{i \in \{3,4\}} \sum_{j=2Z+1}^n \mu_j^{(i)}$.

Ideally, we want to find an optimal solution associated with $\mathcal{L}_{\text{total,lb}}$, but $\mathcal{L}_{\text{total,lb}}$ may not be always achievable. Hence in the next two subsections, we focus on exploring the necessary conditions and sufficient conditions for $\mathcal{L}_{\text{total}}^* = \mathcal{L}_{\text{total,lb}}$.

For further analysis, $\forall i \in \{3, 4\}$, we define

$$U^{(i)} = [u_1^{(i)}, u_2^{(i)}, \dots, u_{\min\{2Z, n\}}^{(i)}] \in \mathbb{R}^{n \times \min\{2Z, n\}},$$

where the column vectors of $U^{(i)}$ are the top- $\min\{2Z, n\}$ normalized eigen-vectors of $S^{(i)}$. Making $\text{col}(U^{(3)}) \subseteq \text{col}([\Phi^{(1,3)}, \Phi^{(5,6)}])$ and $\text{col}(U^{(4)}) \subseteq \text{col}([\Phi^{(2,4)}, \Phi^{(5,6)}])$ is one way to achieve $\mathcal{L}_{\text{total,lb}}$. Moreover, we let $U^{(1)} \in \mathbb{R}^{n \times a}$ and $U^{(2)} \in \mathbb{R}^{n \times b}$ be matrices whose column vectors are the first a and last b column vectors of matrix L , respectively. The network topology constrains $\text{col}(\Phi^{(1,3)}), \text{col}(\Phi^{(1,5)}) \subseteq \text{col}(U^{(1)})$ and $\text{col}(\Phi^{(2,4)}), \text{col}(\Phi^{(2,5)}) \subseteq \text{col}(U^{(2)})$. Therefore, we say $\Phi^{(1,3)}$ is *valid* if $\text{col}(\Phi^{(1,3)}) \subseteq \text{col}(U^{(1)})$, and $\Phi^{(2,4)}$ is *valid* if $\text{col}(\Phi^{(2,4)}) \subseteq \text{col}(U^{(2)})$. On the other hand, any $\Phi^{(5,6)}$ is valid, since $\forall \Phi^{(5,6)} \in \mathbb{R}^{n \times Z}, \exists \Phi^{(1,5)}, \Phi^{(2,5)}$ and $E^{(5,6)}$ s.t. $\Phi^{(5,6)\top} = E^{(5,6)\top} [\Phi^{(1,5)}, \Phi^{(2,5)}]^\top$, $\text{col}(\Phi^{(1,5)}) \subseteq \text{col}(U^{(1)})$, and $\text{col}(\Phi^{(2,5)}) \subseteq \text{col}(U^{(2)})$.

Furthermore, we also let $r_+^{(i,j)} = \dim(\text{col}([U^{(i)}, U^{(j)}]))$ and $r_-^{(i,j)} = \dim(\text{col}(U^{(i)} \cap \text{col}(U^{(j)})))$, $\forall i, j \in \{1, 2, 3, 4\}$, where $\dim(\cdot)$ is the dimension of a vector space.

4.2. Necessary condition

The following Theorem 4.2 provides a necessary condition for achieving $\mathcal{L}_{\text{total,lb}}$ under a mild assumption.

Theorem 4.2. Assume the eigen-gap $\mu_{2Z}^{(i)} - \mu_{2Z+1}^{(i)} > 0$ (define $\mu_{n+1}^{(i)} = 0$), $\forall i \in \{3, 4\}$. Then $\mathcal{L}_{\text{total,lb}}$ is achiev-

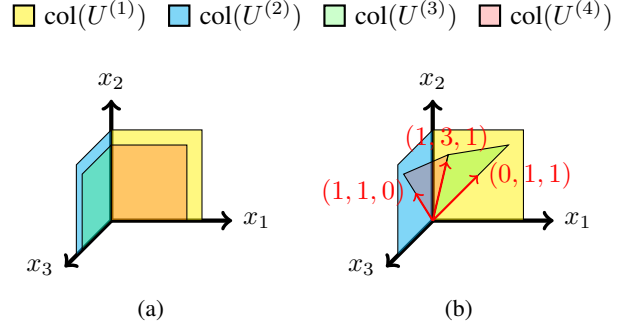


Figure 2. Two illustrative examples for Theorem 4.2, where the left one doesn't achieve $\mathcal{L}_{\text{total,lb}}$ while the right one does.

able only when $r_+^{(3,4)} \leq 3Z$, $r_-^{(1,3)} \geq \min\{Z, n - Z\}$ and $r_-^{(2,4)} \geq \min\{Z, n - Z\}$.

Proof. If the eigen-gap $\mu_{2Z}^{(i)} - \mu_{2Z+1}^{(i)} > 0, \forall i \in \{3, 4\}$, then according to the discussion in Sec. 2, $\mathcal{L}_{\text{total,lb}}$ is achievable only when $\text{col}([\Phi^{(1,3)}, \Phi^{(5,6)}]) = \text{col}(U^{(3)})$ and $\text{col}([\Phi^{(2,4)}, \Phi^{(5,6)}]) = \text{col}(U^{(4)})$, which further implies $\text{col}([\Phi^{(1,3)}, \Phi^{(2,4)}, \Phi^{(5,6)}]) = \text{col}([U^{(3)}, U^{(4)}])$.

Notice that $\dim(\text{col}([\Phi^{(1,3)}, \Phi^{(2,4)}, \Phi^{(5,6)}])) \leq 3Z$. Thus when $r_+^{(3,4)} > 3Z$ it is impossible to make $\text{col}([\Phi^{(1,3)}, \Phi^{(2,4)}, \Phi^{(5,6)}]) = \text{col}([U^{(3)}, U^{(4)}])$. Hence $\mathcal{L}_{\text{total,lb}}$ is not achievable.

Moreover, if $r_-^{(1,3)} < \min\{Z, n - Z\}$, then $\dim(\text{col}([\Phi^{(1,3)}, \Phi^{(5,6)}])) \leq r_-^{(1,3)} + Z < \min\{2Z, n\} = \dim(\text{col}(U^{(3)}))$, which means we cannot make $\text{col}([\Phi^{(1,3)}, \Phi^{(5,6)}]) = \text{col}(U^{(3)})$. So $\mathcal{L}_{\text{total,lb}}$ is not achievable. Similarly, $\mathcal{L}_{\text{total,lb}}$ is not achievable when $r_-^{(2,4)} < \min\{Z, n - Z\}$. \square

To show the conditions in Theorem 4.2 are only necessary but not sufficient, we present two examples in Fig. 2, where the left one doesn't achieve $\mathcal{L}_{\text{total,lb}}$ while the right one does. Here we have $n = 3, \Psi = I, Z = 1, a = b = 2$. And we also assume eigen-gap $\mu_2^{(i)} - \mu_3^{(i)} > 0, \forall i \in \{3, 4\}$. Therefore, to achieve $\mathcal{L}_{\text{total,lb}}$, we must have $\text{col}([\Phi^{(1,3)}, \Phi^{(5,6)}]) = \text{col}(U^{(3)})$ and $\text{col}([\Phi^{(2,4)}, \Phi^{(5,6)}]) = \text{col}(U^{(4)})$. In Fig. 2(a), we assume $u_1^{(3)} = u_1^{(4)} = [0, 1, 0]^\top, u_2^{(3)} = [0, 0, 1]^\top$ and $u_2^{(4)} = [1, 0, 0]^\top$. So we have $r_+^{(3,4)} = 3$ and $r_-^{(1,3)} = r_-^{(1,4)} = 1$. The conditions in Theorem 4.2 are satisfied, but we cannot make $\text{col}([\Phi^{(1,3)}, \Phi^{(5,6)}]) = \text{col}(U^{(3)})$ and $\text{col}([\Phi^{(2,4)}, \Phi^{(5,6)}]) = \text{col}(U^{(4)})$ simultaneously, and hence $\mathcal{L}_{\text{total,lb}}$ is not achievable. In Fig. 2(b), we assume $u_1^{(3)} = u_1^{(4)} = \frac{1}{\sqrt{11}}[1, 1, 3]^\top, u_2^{(3)} = \frac{1}{\sqrt{66}}[4, -7, 1]^\top$ and $u_2^{(4)} = \frac{1}{\sqrt{66}}[-7, 4, 1]^\top$. For $\Phi^{(1,3)} = [0, 1, 1]^\top$,

$\Phi^{(2,4)} = [1, 0, 1]^\top$ and $\Phi^{(5,6)} = [1, 3, 1]^\top$, $\mathcal{L}_{\text{total,lb}}$ is achievable because $\text{col}([\Phi^{(1,3)}, \Phi^{(5,6)}]) = \text{col}(U^{(3)})$ and $\text{col}([\Phi^{(2,4)}, \Phi^{(5,6)}]) = \text{col}(U^{(4)})$.

4.3. Sufficient Conditions

In this subsection we give a few different sufficient conditions related to the parameters $n, a, b, Z, K^{(3)}, K^{(4)}$ for achieving $\mathcal{L}_{\text{total,lb}}$. Note that $n, Z, K^{(3)}, K^{(4)}$ determine $U^{(3)}$ and $U^{(4)}$. The overall result is summarized in Table 1. Fundamentally, the listed sufficient conditions make $\text{col}(U^{(3)}) \subseteq \text{col}([\Phi^{(1,3)}, \Phi^{(5,6)}])$ and $\text{col}(U^{(4)}) \subseteq \text{col}([\Phi^{(2,4)}, \Phi^{(5,6)}])$ possible, which hence guarantees the achievability of $\mathcal{L}_{\text{total,lb}}$. We will give detailed proofs to Theorem 4.3 and 4.7, which do not make assumptions on the observations and tasks and consider the general case. Other corollaries are their natural corollaries with some assumptions on the observations or tasks.

First, for Theorem 4.3 and 4.7, they both require $\text{col}(U^{(3)}) = \text{span}((\text{col}(U^{(1)}) \cap \text{col}(U^{(3)})) \cup (\text{col}(U^{(3)}) \cap \text{col}(U^{(4)})))$. It implies that we can find $\min\{2Z, n\} - r_{-}^{(3,4)}$ vectors in $\text{col}(U^{(1)}) \cap \text{col}(U^{(3)}) \subseteq \text{col}(U^{(1)})$ that extend a basis of $\text{col}(U^{(3)}) \cap \text{col}(U^{(4)})$ to a basis of $\text{col}(U^{(3)})$. Similarly, we can find $\min\{2Z, n\} - r_{-}^{(3,4)}$ vectors in $\text{col}(U^{(2)})$ that extend a basis of $\text{col}(U^{(3)}) \cap \text{col}(U^{(4)})$ to a basis of $\text{col}(U^{(4)})$. As a result, we can find $r_{+}^{(3,4)}$ vectors, denoted by $v_1, \dots, v_{r_{+}^{(3,4)}}$, such that $v_1, \dots, v_{\min\{2Z, n\}}$ and $v_{r_{+}^{(3,4)} - \min\{2Z, n\} + 1}, \dots, v_{r_{+}^{(3,4)}}$ form bases of $\text{col}\{U^{(3)}\}$ and $\text{col}\{U^{(4)}\}$, respectively; $v_{r_{+}^{(3,4)} - \min\{2Z, n\} + 1}, \dots, v_{\min\{2Z, n\}}$ form a basis of $\text{col}\{U^{(3)}\} \cap \text{col}\{U^{(4)}\}$; and

$$\begin{aligned} v_1, \dots, v_{r_{+}^{(3,4)} - \min\{2Z, n\}} &\in \text{col}(U^{(1)}), \\ v_{\min\{2Z, n\} + 1}, \dots, v_{r_{+}^{(3,4)}} &\in \text{col}(U^{(2)}). \end{aligned}$$

We now proceed to the detailed proofs of Theorem 4.3 and 4.7, which are based on the constructed vectors $v_1, \dots, v_{r_{+}^{(3,4)}}$.

Theorem 4.3. *If 1) $r_{+}^{(3,4)} \leq 3Z$, $\text{col}(U^{(3)}) = \text{span}((\text{col}(U^{(1)}) \cap \text{col}(U^{(3)})) \cup (\text{col}(U^{(3)}) \cap \text{col}(U^{(4)})))$, $\text{col}(U^{(4)}) = \text{span}((\text{col}(U^{(2)}) \cap \text{col}(U^{(4)})) \cup (\text{col}(U^{(3)}) \cap \text{col}(U^{(4)})))$, and 2a) $\text{col}(U^{(3)}) \cap \text{col}(U^{(4)}) \subseteq \text{col}(U^{(1)}) \cap \text{col}(U^{(2)})$, then $\mathcal{L}_{\text{total,lb}}$ is achievable.*

Proof. Since $r_{+}^{(3,4)} \leq 3Z$, we have $r_{-}^{(3,4)} \geq Z$ (if $2Z > n$, we have $r_{-}^{(3,4)} = n \geq Z$; else $r_{-}^{(3,4)} \geq 2 \times 2Z - r_{+}^{(3,4)} \geq Z$). We first randomly choose Z vectors in $v_{r_{+}^{(3,4)} - \min\{2Z, n\} + 1}, \dots, v_{\min\{2Z, n\}}$ to be the column vectors of $\Phi^{(5,6)}$. We then let the first $\min\{Z, n - Z\}$ col-

umn vectors of $\Phi^{(1,3)}$ be the rest $\min\{Z, n - Z\}$ vectors in $v_1, \dots, v_{\min\{2Z, n\}}$, and if $n < 2Z$, we let the rest $2Z - n$ column vectors of $\Phi^{(1,3)}$ be arbitrary vectors in $\text{col}(U^{(1)})$. Since $\text{col}(U^{(3)}) \subseteq \text{col}(U^{(1)})$, such $\Phi^{(1,3)}$ is valid. And we can similarly construct $\Phi^{(2,4)}$. It can be verified that $\text{col}([\Phi^{(1,3)}, \Phi^{(5,6)}]) = \text{col}(U^{(3)})$ and $\text{col}([\Phi^{(2,4)}, \Phi^{(5,6)}]) = \text{col}(U^{(4)})$, which means $\mathcal{L}_{\text{total,lb}}$ is achievable. \square

Corollary 4.4. *If $a = b = n$, i.e., the observations are the same, and $r_{+}^{(3,4)} \leq 3Z$, then $\mathcal{L}_{\text{total,lb}}$ is achievable.*

Proof. $a = b = n$ is equivalent to $\text{col}(U^{(1)}) = \text{col}(U^{(2)}) = \mathbb{R}^n$, and hence implies $\text{col}(U^{(3)}) = \text{span}((\text{col}(U^{(1)}) \cap \text{col}(U^{(3)})) \cup (\text{col}(U^{(3)}) \cap \text{col}(U^{(4)})))$, $\text{col}(U^{(4)}) = \text{span}((\text{col}(U^{(2)}) \cap \text{col}(U^{(4)})) \cup (\text{col}(U^{(3)}) \cap \text{col}(U^{(4)})))$, and condition 2a. \square

Corollary 4.5. *If $S^{(3)} = S^{(4)}$, i.e., the tasks are the same, and $\text{col}(U^{(3)}) \subseteq \text{col}(U^{(1)}) \cap \text{col}(U^{(2)})$, then $\mathcal{L}_{\text{total,lb}}$ is achievable.*

Proof. $S^{(3)} = S^{(4)}$ is equivalent to $\text{col}(U^{(3)}) \cap \text{col}(U^{(4)}) = \text{col}(U^{(3)}) = \text{col}(U^{(4)})$, and hence implies condition 1. \square

Corollary 4.6. *If $a = b = n$ and $S^{(3)} = S^{(4)}$, i.e., the observations and the tasks are the same, $\mathcal{L}_{\text{total,lb}}$ is achievable.*

Proof. Combine proofs for Corollary 4.4 and 4.5. \square

Theorem 4.7. *If 1) $r_{+}^{(3,4)} \leq 3Z$, $\text{col}(U^{(3)}) = \text{span}((\text{col}(U^{(1)}) \cap \text{col}(U^{(3)})) \cup (\text{col}(U^{(3)}) \cap \text{col}(U^{(4)})))$, $\text{col}(U^{(4)}) = \text{span}((\text{col}(U^{(2)}) \cap \text{col}(U^{(4)})) \cup (\text{col}(U^{(3)}) \cap \text{col}(U^{(4)})))$, and 2b) $n \leq Z + \min\{a, b\}$, then $\mathcal{L}_{\text{total,lb}}$ is achievable.*

For the sake of clarity, we only provide the proof of Theorem 4.7 when $2Z \leq n$. The proof idea when $2Z > n$ is quite similar and we put it in Sec. A.3 due to space limit.

Proof. Suppose $2Z \leq n$. We start with a matrix $W \in \mathbb{R}^{r_{-}^{(3,4)} \times n}$. We initialize the column vectors of W^\top by $v_{r_{+}^{(3,4)} - 2Z + 1}, \dots, v_{2Z}$, and then do transformations on W , as shown in Fig. 3. There are three major steps:

I) We put columns $a + 1 : n$ before columns $n - b + 1 : a$, and then perform Gauss-Jordan elimination for W . We get W 's reduced row echelon form, which has the following two properties: i) The leading coefficient of a nonzero row is always strictly to the right of the leading coefficient of the row above it, and is always 1 (called a leading 1); ii) Each column containing a leading 1 has zeros in all its other entries. Therefore, W now must have the form as shown in Fig. 3 after Step I, where a' and b' are integers such that $a \leq a' \leq n$, $b \leq b' \leq n$, and $a' - a$ and $b' - b$ are the

Table 1. Sufficient conditions for achieving $\mathcal{L}_{\text{total,lb}}$.

Observations	Tasks	
	Same ($S^{(3)} = S^{(4)}$)	Not Same
Same ($a = b = n$)	Corollary 4.6: Always achievable	Corollary 4.4: $r_+^{(3,4)} \leq 3Z$
Not Same	Corollary 4.5: $\text{col}(U^{(3)}) \subseteq$ $\text{col}(U^{(1)}) \cap \text{col}(U^{(2)});$ or Corollary 4.8: $n \leq Z + \min\{a, b\}$	The following 1 and 2a (Theorem 4.3) or 1 and 2b (Theorem 4.7): 1) $r_+^{(3,4)} \leq 3Z,$ $\text{col}(U^{(3)}) = \text{span}((\text{col}(U^{(1)}) \cap \text{col}(U^{(3)})) \cup (\text{col}(U^{(3)}) \cap \text{col}(U^{(4)}))),$ $\text{col}(U^{(4)}) = \text{span}((\text{col}(U^{(2)}) \cap \text{col}(U^{(4)})) \cup (\text{col}(U^{(3)}) \cap \text{col}(U^{(4)})));$ 2a) $\text{col}(U^{(3)}) \cap \text{col}(U^{(4)}) \subseteq \text{col}(U^{(1)}) \cap \text{col}(U^{(2)});$ 2b) $n \leq Z + \min\{a, b\}.$

$$\begin{array}{c}
 W = \begin{bmatrix} v_{r_+^{(3,4)}-2Z+1}^\top \\ v_{r_+^{(3,4)}-2Z+2}^\top \\ \vdots \\ v_{2Z}^\top \end{bmatrix} \xrightarrow[\substack{\text{Step I: put columns } a+1:n \text{ before} \\ n-b+1:a, \text{ Gauss-Jordan elimination}}]{\substack{n-b'\{ \\ n-a'\{ \\ r_-^{(3,4)}+a'+b'-2n\{}}}} \begin{bmatrix} * & * & * \\ 0 & * & * \\ 0 & 0 & * \end{bmatrix} \xrightarrow[\substack{\text{Step II: put columns} \\ a+1:n \text{ before } 1:n-b,}]{\substack{1:n-b \quad a+1:n \quad n-b+1:a}} \\
 \\
 \xrightarrow[\substack{\text{Gauss-Jordan elimination} \\ \text{for the first } n-b' \text{ rows}}]{\substack{\min\{a'-a, n-b'\}\{ \\ \max\{n-b'-a'+a, 0\}\{ \\ n-a'\{ \\ r_-^{(3,4)}+a'+b'-2n\{}}}} \begin{bmatrix} * & * & * \\ 0 & * & * \\ * & 0 & * \\ 0 & 0 & * \end{bmatrix} \xrightarrow[\text{rearrange}]{\text{Step III}} \begin{bmatrix} * & * & * \\ * & * & 0 \\ 0 & * & * \\ 0 & * & 0 \end{bmatrix} \begin{array}{l} \leftarrow G_1 \\ \leftarrow G_2 \\ \leftarrow G_3 \\ \leftarrow G_4 \end{array} \\
 \\
 \substack{a+1:n \quad 1:n-b \quad n-b+1:a} \qquad \qquad \qquad \substack{1:n-b \quad n-b+1:a \quad a+1:n}
 \end{array}$$

Figure 3. Explanation for the proof of Theorem 4.7. Here 0 and * represent submatrices that must and may not contain only zero elements, respectively. The notations at the bottom represent the column indices, and the notations on the left represent the number of rows.

number of columns among columns $a+1:n$ and $1:n-b$ that do not have a leading 1, respectively. We also have $r_-^{(3,4)} + a' + b' - 2n \geq 0$.

II) We put columns $a+1:n$ before columns $1:n-b$, and then perform Gauss-Jordan elimination for the first $n-b'$ rows. W now has the form as shown in Fig. 3 after Step II.

III) We rearrange the columns in their original order. W now has the form as shown in Fig. 3 after Step IV. And for convenience of further analysis, we divide the column vectors of W^\top into 4 groups denoted by G_1, G_2, G_3 and G_4 respectively. We have $|G_1| = \min\{a'-a, n-b'\}$, $|G_2| = \max\{n-b'-a'+a, 0\}$, $|G_3| = n-a'$, $|G_4| = r_-^{(3,4)} + a' + b' - 2n$, and $|G_1| + \max\{|G_2|, |G_3|\} \leq n - \min\{a, b\} \leq Z$. Furthermore, after the whole transformation, $\text{col}(W^\top) = \text{col}(U^{(3)}) \cap \text{col}(U^{(4)})$ remains unchanged.

Now we construct $\Phi^{(1,3)}$, $\Phi^{(2,4)}$ and $\Phi^{(5,6)}$ through the following two steps (step ii has two possibilities):

i) Let the first $r_+^{(3,4)} - 2Z$ column vectors of $\Phi^{(1,3)}$ and $\Phi^{(2,4)}$ be $v_1, \dots, v_{r_+^{(3,4)}-2Z}$ and $v_{2Z+1}, \dots, v_{r_+^{(3,4)}}$ respec-

tively, and the first $|G_1|$ column vectors of $\Phi^{(5,6)}$ be the vectors in G_1 ;

ii.a) If $\min\{|G_2|, |G_3|\} > 3Z - r_+^{(3,4)}$, then let the non-determined column vectors of $\Phi^{(1,3)}$ and $\Phi^{(2,4)}$ be the first $3Z - r_+^{(3,4)}$ vectors in G_2 and G_3 respectively. Next let $3Z - r_+^{(3,4)}$ non-determined column vectors of $\Phi^{(5,6)}$ be the pair-wise sums¹ of the first $3Z - r_+^{(3,4)}$ vectors in G_2 and G_3 . Finally let the remaining non-determined column vectors of $\Phi^{(5,6)}$ be the remaining vectors in G_2, G_3, G_4 ;

ii.b) If $\min\{|G_2|, |G_3|\} \leq 3Z - r_+^{(3,4)}$, then let $\min\{|G_2|, |G_3|\}$ non-determined column vectors of $\Phi^{(1,3)}$ and $\Phi^{(2,4)}$ be the first $\min\{|G_2|, |G_3|\}$ vectors in G_2 and G_3 respectively. Next let $\min\{|G_2|, |G_3|\}$ non-determined column vectors of $\Phi^{(5,6)}$ be the pair-wise sums of the first $\min\{|G_2|, |G_3|\}$ vectors in G_2 and G_3 , and another

¹Here pair-wise sums of vectors $\xi_1, \xi_2, \dots, \xi_p$ and vectors $\chi_1, \chi_2, \dots, \chi_p$ are vectors $\xi_1 + \chi_1, \xi_2 + \chi_2, \dots, \xi_p + \chi_p$. With vectors $\xi_1, \xi_2, \dots, \xi_p$ and vectors $\xi_1 + \chi_1, \xi_2 + \chi_2, \dots, \xi_p + \chi_p$, one can decode vectors $\chi_1, \chi_2, \dots, \chi_p$ through $\chi_i = -\xi_i + (\xi_i + \chi_i), \forall i \in \{1, 2, \dots, p\}$.

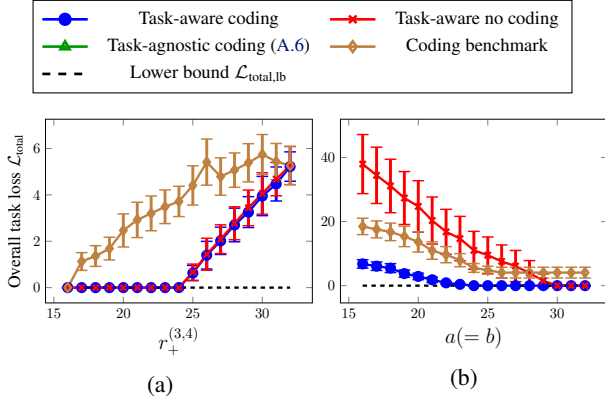


Figure 4. Simulation result with synthetic data: overall task loss $\mathcal{L}_{\text{total}}$ under different $r_+^{(3,4)}$ (left) and different a (right). The task losses for task-agnostic coding are too large and have to be put in a separate figure in Sec. A.6.

$\max\{|G_2|, |G_3|\} - \min\{|G_2|, |G_3|\}$ non-determined column vectors of $\Phi^{(5,6)}$ be the remaining vectors in G_2 or G_3 . Finally let the remaining non-determined column vectors of $\Phi^{(5,6)}$ be the first $Z - |G_1| - \max\{|G_2|, |G_3|\}$ vectors in G_4 , and the remaining non-determined column vectors of $\Phi^{(1,3)}$ and $\Phi^{(2,4)}$ both be the remaining vectors in G_4 .

According to the formats of the vectors in different groups as in Fig. 3, the constructed $\Phi^{(1,3)}$ and $\Phi^{(2,4)}$ are valid, and we also have $\text{col}([\Phi^{(1,3)}, \Phi^{(5,6)}]) = \text{col}(U^{(3)})$ and $\text{col}([\Phi^{(2,4)}, \Phi^{(5,6)}]) = \text{col}(U^{(4)})$. Therefore, $\mathcal{L}_{\text{total,lb}}$ is achievable. \square

Corollary 4.8. *If $S^{(3)} = S^{(4)}$, i.e., the tasks are the same, and $n \leq Z + \min\{a, b\}$, then $\mathcal{L}_{\text{total,lb}}$ is achievable.*

Proof. Same as the proof for Corollary 4.5. \square

5. Algorithm

In Sec. 4.3 we have discussed the sufficient conditions for achieving $\mathcal{L}_{\text{total,lb}}$, and corresponding optimal encoder and decoder parameters can be determined analytically. In the general case when these sufficient conditions are not satisfied, we resort to standard machine learning algorithm to determine the encoder and decoder parameters jointly. We initialize encoder and decoder parameters randomly and update them for multiple epochs. In each epoch, we update $E^{(i,j)}$ and $D^{(i)}$ through back-propagation as follows:

$$E^{(i,j)} \leftarrow E^{(i,j)} - \eta \frac{\nabla \mathcal{L}_{\text{total}}}{\nabla E^{(i,j)}}, \quad \forall (i,j) \in \mathcal{E}' \quad (10)$$

$$D^{(i)} \leftarrow D^{(i)} - \eta \frac{\nabla \mathcal{L}_{\text{total}}}{\nabla D^{(i)}}, \quad \forall i \in \{3, 4\} \quad (11)$$

where η is the learning rate.

To show our algorithm converges to near-optimal solution for low-dimensional data and to verify our conclusions in Sec. 4.3 numerically, we run simulation with synthetic data for our task-aware coding approach and compare against three benchmark approaches. The benchmark approaches are: 1) **Task-aware no coding** approach, where network coding at node 5 is not allowed, i.e., each dimension of $\phi^{(5,6)}$ can only be a dimension of $\phi^{(1,5)}$ or $\phi^{(2,5)}$; 2) **Task-agnostic coding** approach (used in Liu et al. (2020)), where the objective is to minimize the reconstruction loss at node 3 and 4, i.e., $K^{(3)} = K^{(4)} = I$; 3) **Task-aware coding benchmark** (abbreviated as **coding benchmark**) approach, which is also a task-aware coding approach but the encoder parameters associated with edge (5, 6) is determined greedily first and then other parameters. Such greedy approach doesn't ensure global optimality but provides a general analytical solution (see Sec. A.4 for further details).

The simulation results are shown in Fig. 4. The parameters are as follows: we fix $n = 32$, $\Psi = I$, $a = b \geq 16$, $Z = 8$. Next we let eigen-values $\mu_1^{(3)}, \dots, \mu_{2Z}^{(3)}$ and $\mu_1^{(4)}, \dots, \mu_{2Z}^{(4)}$ be positive, and other eigen-values of $S^{(3)}$ and $S^{(4)}$ be 0. Hence $\mathcal{L}_{\text{total,lb}} = 0$. Other training details are provided in Sec. A.5. In Fig. 4(a), we fix $a = b = 24$ and change eigen-vectors $u_1^{(3)}, \dots, u_{2Z}^{(3)}$ and $u_1^{(4)}, \dots, u_{2Z}^{(4)}$ to make $r_+^{(3,4)}$ different, while in the meantime keep $\text{col}(U^{(3)}) = \text{span}((\text{col}(U^{(1)}) \cap \text{col}(U^{(3)})) \cup (\text{col}(U^{(3)}) \cap \text{col}(U^{(4)})))$, $\text{col}(U^{(4)}) = \text{span}((\text{col}(U^{(2)}) \cap \text{col}(U^{(4)})) \cup (\text{col}(U^{(3)}) \cap \text{col}(U^{(4)})))$ and $\text{col}(U^{(3)}) \cap \text{col}(U^{(4)}) \subseteq \text{col}(U^{(1)}) \cap \text{col}(U^{(2)})$. We can see that our task-aware coding approach achieves $\mathcal{L}_{\text{total,lb}}$ when $r_+^{(3,4)} \leq 24$, which verifies our conclusion in Theorem 4.3. We also notice that the task-aware no coding approach achieves $\mathcal{L}_{\text{total,lb}}$ when $r_+^{(3,4)} \leq 24$ as well, since coding is not required to achieve $\mathcal{L}_{\text{total,lb}}$ according to the proof of Theorem 4.3. In Fig. 4(b), we fix $u_1^{(3)}, \dots, u_{2Z}^{(3)}$ and $u_1^{(4)}, \dots, u_{2Z}^{(4)}$ such that $r_+^{(3,4)} = 18$, and change a , while in the meantime keep $\text{col}(U^{(3)}) = \text{span}((\text{col}(U^{(1)}) \cap \text{col}(U^{(3)})) \cup (\text{col}(U^{(3)}) \cap \text{col}(U^{(4)})))$ and $\text{col}(U^{(4)}) = \text{span}((\text{col}(U^{(2)}) \cap \text{col}(U^{(4)})) \cup (\text{col}(U^{(3)}) \cap \text{col}(U^{(4)})))$. We can see that our task-aware coding approach achieves $\mathcal{L}_{\text{total,lb}}$ when $a = b \geq 24$, which verifies our conclusion in Theorem 4.7. Furthermore, in both Fig. 4(a) and 4(b), our task-aware coding approach beats all the other benchmark approaches under varying $r_+^{(3,4)}$'s with respect to overall task loss $\mathcal{L}_{\text{total}}$.

In the next section we will evaluate our approach over a high-dimensional real-world dataset.

6. Evaluation

Our evaluation compares the performance of our task-aware coding approach and other benchmark approaches (as in Sec. 5) over MNIST dataset (LeCun et al., 1998), where each

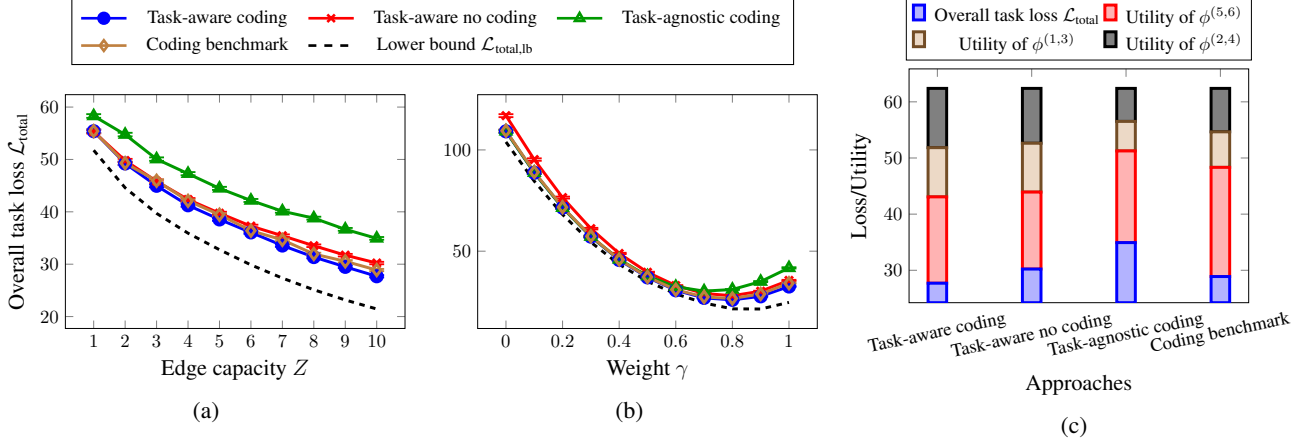


Figure 5. Evaluation result with MNIST dataset. Left: overall task loss $\mathcal{L}_{\text{total}}$ under different edge capacity Z (with $\gamma = 0.9$). Middle: overall task loss $\mathcal{L}_{\text{total}}$ under different weight γ (with $Z = 10$). Right: comparison of the utilities of $\phi^{(5,6)}$, $\phi^{(1,3)}$ and $\phi^{(2,4)}$ for different approaches (with $Z = 10$ and $\gamma = 0.9$).

data sample is a 28×28 handwritten digit image. In our evaluation, we let x be a horizontally-concatenated image (28×56) of two MNIST images, i.e., $n = 1568$. Node 1 and 2 observe the upper and the lower half part of the concatenated image (both 14×56) respectively, i.e., $a = b = 784$. Task matrices $K^{(3)}$ and $K^{(4)}$ are formulated as follows: we pre-train a convolutional neural network (CNN) to classify original MNIST digits by their labels. Task matrix $K^{(3)}$ requires both the reconstruction of the feature map (i.e., the output of the first layer of CNN) of the left MNIST digit in the concatenated image, and the reconstruction of the concatenated image itself. Mathematically, we have

$$K^{(3)} = \begin{bmatrix} \underbrace{\gamma \tilde{K}^{(3)\top}}_{\text{recon. of left feature map}} & , & \underbrace{(1-\gamma)I}_{\text{recon. of concatenated image}} \end{bmatrix}^\top, \quad (12)$$

where $\tilde{K}^{(3)}$ represents the mapping between x and the feature map of the left MNIST digit, and $\gamma \in [0, 1]$ is a weight coefficient. Task matrix $K^{(4)}$ is formulated similarly while the feature map of the right MNIST digit is considered instead. Other training details are provided in Sec. A.5.

The evaluation result is shown in Fig. 5. In Fig. 5(a) and Fig. 5(b), we plot the overall task loss $\mathcal{L}_{\text{total}}$ under different edge capacity Z (with $\gamma = 0.9$) and different weight γ (with $Z = 10$) for different approaches, respectively. In both figures, we see task-aware coding approaches (i.e., task-aware coding and coding benchmark approach) outperform task-aware no coding and task-agnostic coding approach, and the overall task loss $\mathcal{L}_{\text{total}}$ of our task-aware coding approach is the closest to $\mathcal{L}_{\text{total,lb}}$. And in Fig. 5(b) we see the curves for our task-aware coding approach and task-agnostic coding approach nearly overlap when γ is small, since $K^{(3)}$ and $K^{(4)}$ for our task-aware coding approach are both dominated by the reconstruction of the concatenated image itself. On the

other hand, when γ is big we observe clear improvement of overall task loss $\mathcal{L}_{\text{total}}$ for task-aware coding approach compared to task-agnostic coding approach, which is as large as 28.2% when $\gamma = 1$. This illustrates the benefit of making the network coding task-aware.

In Fig. 5(c), we compare the utilities of $\phi^{(5,6)}$, $\phi^{(1,3)}$ and $\phi^{(2,4)}$ in terms of minimizing the overall task loss $\mathcal{L}_{\text{total}}$ when $Z = 10$, $\gamma = 0.9$. The three utilities are defined in a way such that their sums plus $\mathcal{L}_{\text{total}}$ is a fixed number, as in Sec. A.7. We observe that the coding benchmark approach outperforms other approaches with respect to the utility of $\phi^{(5,6)}$, but underperforms our task-aware coding approach by 4.2% with respect to the overall task loss $\mathcal{L}_{\text{total}}$. This is because coding benchmark approach greedily determines the encoder parameters associated with edge (5, 6) first which however could not guarantee optimality. On the other hand, our task-aware coding approach tunes all the encoding and decoding parameters jointly and achieves a lower $\mathcal{L}_{\text{total}}$.

7. Conclusion

This paper considers task-aware network coding over butterfly network in real-coordinate space. We prove a lower bound $\mathcal{L}_{\text{total,lb}}$ of the total loss, as well as conditions for achieving $\mathcal{L}_{\text{total,lb}}$. We also provide a machine learning algorithm in the general settings. Experimental results demonstrate that our task-aware coding approach outperforms the benchmark approaches under various settings.

Regarding future extension, although butterfly network is a representative topology in network coding, it is worthwhile to extend the analysis of the task-aware network coding problem to general networks. A similar $\mathcal{L}_{\text{total,lb}}$ can still be derived, yet the associated necessary condition and suffi-

cient conditions for achieving $\mathcal{L}_{\text{total,lb}}$ depend on the specific network topology in a manner that needs further work to be fully understood.

References

- Ahlsvede, R. and Korner, J. Source coding with side information and a converse for degraded broadcast channels. *IEEE Transactions on Information Theory*, 21(6):629–637, 1975.
- Ahlsvede, R., Cai, N., Li, S.-Y., and Yeung, R. W. Network information flow. *IEEE Transactions on information theory*, 46(4):1204–1216, 2000.
- Blau, Y. and Michaeli, T. Rethinking lossy compression: The rate-distortion-perception tradeoff. In *International Conference on Machine Learning*, pp. 675–685. PMLR, 2019.
- Chen, M., Ponc, M., Sengupta, S., Li, J., and Chou, P. A. Utility maximization in peer-to-peer systems. *ACM SIGMETRICS Performance Evaluation Review*, 36(1):169–180, 2008.
- Cheng, J., Pavone, M., Katti, S., Chinchali, S. P., and Tang, A. Data sharing and compression for cooperative networked control. In *Thirty-Fifth Conference on Neural Information Processing Systems*, 2021.
- Doshi, V., Shah, D., Médard, M., and Effros, M. Functional compression through graph coloring. *IEEE Transactions on Information Theory*, 56(8):3901–3917, 2010.
- Dougherty, R., Freiling, C., and Zeger, K. Insufficiency of linear coding in network information flow. *IEEE transactions on information theory*, 51(8):2745–2759, 2005.
- Dubois, Y., Bloem-Reddy, B., Ullrich, K., and Maddison, C. J. Lossy compression for lossless prediction. *arXiv preprint arXiv:2106.10800*, 2021.
- Dunteman, G. H. *Principal components analysis*. Number 69. Sage, 1989.
- Feizi, S. and Médard, M. On network functional compression. *IEEE transactions on information theory*, 60(9):5387–5401, 2014.
- Ho, T., Médard, M., Koetter, R., Karger, D. R., Effros, M., Shi, J., and Leong, B. A random linear network coding approach to multicast. *IEEE Transactions on Information Theory*, 52(10):4413–4430, 2006.
- Jaggi, S., Sanders, P., Chou, P. A., Effros, M., Egnér, S., Jain, K., and Tolhuizen, L. M. Polynomial time algorithms for multicast network code construction. *IEEE Transactions on Information Theory*, 51(6):1973–1982, 2005.
- Koetter, R. and Médard, M. An algebraic approach to network coding. *IEEE/ACM transactions on networking*, 11(5):782–795, 2003.
- Korner, J. and Marton, K. How to encode the modulo-two sum of binary sources (corresp.). *IEEE Transactions on Information Theory*, 25(2):219–221, 1979.
- LeCun, Y., Bottou, L., Bengio, Y., and Haffner, P. Gradient-based learning applied to document recognition. *Proceedings of the IEEE*, 86(11):2278–2324, 1998.
- Li, S.-Y., Yeung, R. W., and Cai, N. Linear network coding. *IEEE transactions on information theory*, 49(2):371–381, 2003.
- Liu, L., Solomon, A., Salamatian, S., and Médard, M. Neural network coding. In *ICC 2020-2020 IEEE International Conference on Communications (ICC)*, pp. 1–6. IEEE, 2020.
- Nakanoya, M., Chinchali, S., Anemogiannis, A., Datta, A., Katti, S., and Pavone, M. Co-design of communication and machine inference for cloud robotics. *Robotics: Science and Systems XVII, Virtual Event*, 2021.
- Shannon, C. The zero error capacity of a noisy channel. *IRE Transactions on Information Theory*, 2(3):8–19, 1956.
- Shannon, C. E. et al. Coding theorems for a discrete source with a fidelity criterion. *IRE Nat. Conv. Rec.*, 4(142-163): 1, 1959.
- Slepian, D. and Wolf, J. Noiseless coding of correlated information sources. *IEEE Transactions on information Theory*, 19(4):471–480, 1973.
- Vasishth, D., Shenoy, J., and Chandra, R. L2d2: Low latency distributed downlink for leo satellites. In *Proceedings of the 2021 ACM SIGCOMM 2021 Conference*, pp. 151–164, 2021.
- Wang, J., Acharya, A., Kim, H., and Dimakis, A. G. Neural distributed source coding. *arXiv preprint arXiv:2106.02797*, 2021.
- Wu, Y. and Verdú, S. Rényi information dimension: Fundamental limits of almost lossless analog compression. *IEEE Transactions on Information Theory*, 56(8):3721–3748, 2010.
- Wyner, A. and Ziv, J. The rate-distortion function for source coding with side information at the decoder. *IEEE Transactions on information Theory*, 22(1):1–10, 1976.
- Zhang, G., Qian, J., Chen, J., and Khisti, A. Universal rate-distortion-perception representations for lossy compression. *arXiv preprint arXiv:2106.10311*, 2021.

A. Appendix

A.1. Task-aware PCA Derivation

We define random variable $h = L^{-1}x \in \mathbb{R}^n$ and $\hat{h} = L^{-1}\hat{x} \in \mathbb{R}^n$. Thus $\mathbb{E}_h[hh^\top] = \mathbb{E}_x[L^{-1}xx^\top L^{-\top}] = I$. And we also define $D_h = L^{-1}D$ and $E_h = EL$.

Then we have

$$\begin{aligned} \mathcal{L} &= \mathbb{E}_x[\|K(x - \hat{x})\|_2^2] = \mathbb{E}_h[\|KL(h - \hat{h})\|_2^2] \\ &= \mathbb{E}_h[\|KL(I - D_h E_h)h\|_2^2] \\ &= \mathbb{E}_h[\text{Tr}(KL(I - D_h E_h)hh^\top(I - D_h E_h)^\top L^\top K^\top)] \\ &= \text{Tr}(KL(I - D_h E_h)(I - D_h E_h)^\top L^\top K^\top) \end{aligned} \quad (13)$$

where $\text{Tr}(\cdot)$ denotes the trace of a matrix. We can verify that $D_h = E_h^\top(E_h E_h^\top)^{-1}$ is a zero point of

$$\frac{\nabla \mathcal{L}}{\nabla D_h} = 2L^\top K^\top KL(D_h E_h - I)E_h^\top. \quad (14)$$

So we plug $D_h = E_h(E_h E_h^\top)^{-1}$ into Eq. 13 and get

$$\mathcal{L} = \text{Tr}(L^\top K^\top KL) - \text{Tr}(L^\top K^\top KLE_h^\top(E_h E_h^\top)^{-1}E_h).$$

Therefore, we should find E_h that maximizes $\text{Tr}(L^\top K^\top KLE_h^\top(E_h E_h^\top)^{-1}E_h)$. Classical PCA dictates that $\text{Tr}(L^\top K^\top KLE_h^\top(E_h E_h^\top)^{-1}E_h) \leq \sum_{i=1}^Z \mu_i$, i.e., $\mathcal{L} \geq \sum_{i=Z+1}^n \mu_i$. And if the eigen-gap $\mu_Z - \mu_{Z+1} > 0$, the equality holds if and only if $\text{col}(E_h^\top) = \text{span}(\{u_1, u_2, \dots, u_Z\})$, which is equivalent to $\text{col}(E^\top) = \text{span}(\{L^{-\top}u_1, L^{-\top}u_2, \dots, L^{-\top}u_Z\})$.

A.2. Proof of Theorem 4.1

Proof. Assume the top- \tilde{n} eigen-values of Ψ are greater than zero, where $\tilde{n} \leq n$. We use $\lambda_1, \dots, \lambda_{\tilde{n}}$ to denote these eigen-values and $q_1, \dots, q_{\tilde{n}}$ to denote the corresponding normalized eigen-vectors. Moreover, we let $\Lambda = \text{diag}(\lambda_1, \dots, \lambda_{\tilde{n}}) \in \mathbb{R}^{\tilde{n} \times \tilde{n}}$ and $Q = [q_1, \dots, q_{\tilde{n}}] \in \mathbb{R}^{n \times \tilde{n}}$.

Consider $\tilde{x} = \Lambda^{-\frac{1}{2}}Q^\top x \in \mathbb{R}^{\tilde{n}}$. We have $\mathbb{E}[\tilde{x}\tilde{x}^\top] = \Lambda^{-\frac{1}{2}}Q^\top \Psi Q \Lambda^{-\frac{1}{2}} = I$. And we also have $x = Q\Lambda^{\frac{1}{2}}\tilde{x}$. For simplicity we let $\Theta = (Q\Lambda^{\frac{1}{2}})^\top$ and use θ_i to denote the i -th column vector of Θ . Let $\Theta_1 = [\theta_1, \dots, \theta_a] \in \mathbb{R}^{\tilde{n} \times (n-a)}$ and $\Theta_2 = [\theta_{n-b+1}, \dots, \theta_n] \in \mathbb{R}^{\tilde{n} \times (n-b)}$, and let $\tilde{a} = \dim(\text{col}(\Theta_1))$ and $\tilde{b} = \dim(\text{col}(\Theta_2))$. Then we have $\dim(\text{col}(\Theta_1) \cap \text{col}(\Theta_2)) = \tilde{a} + \tilde{b} - \tilde{n}$. We can find \tilde{n} vectors that form a basis of $\text{col}(\Theta)$, denoted by $\omega_1, \dots, \omega_{\tilde{n}}$, such that $\omega_1, \dots, \omega_{\tilde{a}}$ and $\omega_{\tilde{n}-\tilde{b}+1}, \dots, \omega_{\tilde{n}}$ form bases of $\text{col}(\Theta_1)$ and $\text{col}(\Theta_2)$ respectively, and $\omega_{\tilde{n}-\tilde{b}+1}, \dots, \omega_{\tilde{a}}$ form a basis of $\text{col}(\Theta_1) \cap \text{col}(\Theta_2)$. Therefore, we let $\tilde{x}' = \Omega^\top \tilde{x}$ where $\Omega = [\omega_1, \dots, \omega_{\tilde{n}}] \in \mathbb{R}^{\tilde{n} \times \tilde{n}}$. And from the construction process we have $\forall i \in \{1, \dots, a\}$, x_i can be expressed as a linear combination of $\tilde{x}'_1, \dots, \tilde{x}'_{\tilde{a}}$; $\forall i \in \{n-b+1, \dots, n\}$, x_i can be expressed as a linear

combination of $\tilde{x}'_{\tilde{n}-\tilde{b}+1}, \dots, \tilde{x}'_{\tilde{n}}$. The same conclusion still holds if we switch n, a, b, x and $\tilde{n}, \tilde{a}, \tilde{b}, \tilde{x}'$.

We define $\tilde{\Psi} = \mathbb{E}[\tilde{x}'\tilde{x}'^\top]$. From the construction process, it is obvious that $\text{rank}(\tilde{\Psi}) = n$. Moreover, $\forall i \in \{3, 4\}$, we define $\tilde{K}^{(i)} = K^{(i)}Q\Lambda^{\frac{1}{2}}\Omega^{-\top} \in \mathbb{R}^{m_i \times \tilde{n}}$, and we have $\tilde{K}^{(i)}\tilde{x}' = K^{(i)}x$. In this way, we transformed *TaskAwareCoding*($n, \Psi, a, b, Z, K^{(3)}, K^{(4)}$) to *TaskAwareCoding*($\tilde{n}, \tilde{\Psi}, \tilde{a}, \tilde{b}, Z, \tilde{K}^{(3)}, \tilde{K}^{(4)}$).

Suppose $\{\tilde{E}^{(i,j)} | \forall (i, j) \in \mathcal{E}'\} \cup \{\tilde{D}^{(i)} | \forall i \in \{3, 4\}\}$ is a solution for *TaskAwareCoding*($\tilde{n}, \tilde{\Psi}, \tilde{a}, \tilde{b}, Z, \tilde{K}^{(3)}, \tilde{K}^{(4)}$). We can find $\{E^{(i,j)} | \forall (i, j) \in \mathcal{E}'\} \cup \{D^{(i)} | \forall i \in \{3, 4\}\}$ for *TaskAwareCoding*($n, \Psi, a, b, Z, K^{(3)}, K^{(4)}$), such that $\phi^{(i,j)} = \tilde{\phi}^{(i,j)}$, $\forall (i, j) \in \mathcal{E}$. For encoder parameters $\{E^{(i,j)} | \forall (i, j) \in \mathcal{E}'\}$, we take $E^{(1,3)}$ as an example. We let $E^{(1,3)} = \tilde{E}^{(1,3)}M$ where $M \in \mathbb{R}^{\tilde{a} \times a}$ represents a linear transformation from x_1, \dots, x_a to $\tilde{x}'_1, \dots, \tilde{x}'_{\tilde{a}}$. Moreover, for decoder parameters we let $D^{(i)} = Q\Lambda^{\frac{1}{2}}\Omega^{-\top}\tilde{D}^{(i)}$, $\forall i \in \{3, 4\}$. Therefore, $\forall i \in \{3, 4\}$, we have $\tilde{K}^{(i)}\tilde{x}' = K^{(i)}\hat{x}$. This implies the associated overall task losses for these two problems with these two sets of encoder and decoder parameters are the same.

Similarly, we can also transform a solution $\{E^{(i,j)} | \forall (i, j) \in \mathcal{E}'\} \cup \{D^{(i)} | \forall i \in \{3, 4\}\}$ for *TaskAwareCoding*($n, \Psi, a, b, Z, K^{(3)}, K^{(4)}$) to a set of parameters $\{\tilde{E}^{(i,j)} | \forall (i, j) \in \mathcal{E}'\} \cup \{\tilde{D}^{(i)} | \forall i \in \{3, 4\}\}$ for *TaskAwareCoding*($\tilde{n}, \tilde{\Psi}, \tilde{a}, \tilde{b}, Z, \tilde{K}^{(3)}, \tilde{K}^{(4)}$), and obtain the same conclusion.

This implies that the optimal overall task losses for these two problems are equal, and the above transformation from an optimal solution for one problem actually yields an optimal solution for the other. \square

A.3. Proof of Theorem 4.7 when $2Z > n$

Proof. When $2Z > n$, we have $r_+^{(3,4)} = n$. Therefore we aim to make $\text{col}([\Phi^{(1,3)}, \Phi^{(5,6)}]) = \text{col}([\Phi^{(2,4)}, \Phi^{(5,6)}]) = \mathbb{R}^n$. Since butterfly network is symmetric, without loss of generality, we assume $a \leq b$. And we denote the i -th column vector of L by l_i .

We are able to find $\Phi^{(1,3)}, \Phi^{(2,4)}$ and $\Phi^{(5,6)}$ such that $\mathcal{L}_{\text{total,lb}}$ is achievable, through the following three steps:

- i) Let the first $n-b$ column vectors of $\Phi^{(5,6)}$ be $l_1 + l_{a+1}, l_2 + l_{a+2}, \dots, l_{n-b} + l_{a+n-b}$, and the next $b-a$ column vectors of $\Phi^{(5,6)}$ be $l_{a+n-b+1}, l_{a+n-b+2}, \dots, l_n$;
- ii) Let the first $n-b$ column vectors of $\Phi^{(1,3)}$ and $\Phi^{(2,4)}$ be l_1, l_2, \dots, l_{n-b} and $l_{a+1}, l_{a+2}, \dots, l_{a+n-b}$ respectively;
- iii) Since $2Z > n$, we have $Z-n+a+Z-n+b > a+b-n$, i.e., the number of non-determined column vectors of $\Phi^{(5,6)}$ and $\Phi^{(1,3)}$ together is greater than the number of remaining vectors $l_{n-b+1}, l_{n-b+2}, \dots, l_a$. So we can as-

sign $l_{n-b+1}, l_{n-b+2}, \dots, l_a$ to the non-determined column vectors of $\Phi^{(5,6)}$ and $\Phi^{(1,3)}$ such that each vector among $l_{n-b+1}, l_{n-b+2}, \dots, l_a$ is assigned at least once. After that we assign the last $Z - n + b$ column vectors of $\Phi^{(1,3)}$ to the last $Z - n + b$ column vectors of $\Phi^{(2,4)}$.

It can be verified that $\text{col}([\Phi^{(1,3)}, \Phi^{(5,6)}]) = \text{col}([\Phi^{(2,4)}, \Phi^{(5,6)}]) = \text{col}(L) = \mathbb{R}^n$. Therefore, $\mathcal{L}_{\text{total,lb}}$ is achievable. \square

A.4. Further explanation of the task-aware coding benchmark approach

In the coding benchmark approach, our first step is to let the column vectors of $\Phi^{(5,6)}$ be the top- Z normalized eigenvectors of $S^{(3)} + S^{(4)}$. This greedy step ensures $\mathcal{L}_{\text{total}}$ is minimized when node 3 and 4 receive $\phi^{(5,6)}$ only.

Next, to determine optimal $\Phi^{(1,3)}$ which further minimizes $\mathcal{L}_{\text{total}}$ as much as possible, we consider the following problem:

$$\max_{\tilde{\Phi}^{(1,3)} \in \mathbb{R}^{n \times \min\{Z, c\}}} \tilde{\Phi}^{(1,3)\top} S^{(3)} \tilde{\Phi}^{(1,3)} \quad (15)$$

$$\text{s.t. } \text{col}(\tilde{\Phi}^{(1,3)}) \subseteq V, \quad (16)$$

$$\tilde{\Phi}^{(1,3)\top} \tilde{\Phi}^{(1,3)} = I, \quad (17)$$

where $V = \{v \in \text{col}([\Phi^{(5,6)}, U^{(1)}]) | v \perp w, \forall w \in \text{col}(\Phi^{(5,6)})\}$, and $c = \dim(\text{col}([\Phi^{(5,6)}, U^{(1)}])) - Z$ is the dimension of V . The following $\tilde{\Phi}^{(1,3)}$ is an optimal solution for the considered problem: we formulate a matrix $W \in \mathbb{R}^{n \times c}$ whose column vectors form an orthogonal basis of V , and then let the column vectors of $\tilde{\Phi}^{(1,3)}$ be W times the top- $\min\{Z, c\}$ normalized eigen-vectors of $W^\top S^{(3)} W$. For fixed $\Phi^{(5,6)}$, we know the optimal $\Phi^{(1,3)}$ that minimizes $\mathcal{L}_{\text{total}}$ should satisfy $\text{col}([\Phi^{(1,3)}, \Phi^{(5,6)}]) = \text{col}([\tilde{\Phi}^{(1,3)}, \Phi^{(5,6)}])$. Yet in general $\tilde{\Phi}^{(1,3)} \notin U^{(1)}$, so we cannot assign the column vectors of $\tilde{\Phi}^{(1,3)}$ to the column vectors of $\Phi^{(1,3)}$ directly. Therefore, we let the first $\min\{Z, c\}$ column vectors of $\Phi^{(1,3)}$ be the vectors in $\text{col}(U^{(1)})$ that extend a basis of $\text{col}(\Phi^{(5,6)})$ to a basis of $\text{col}([\tilde{\Phi}^{(1,3)}, \Phi^{(5,6)}])$. Other non-determined column vectors of $\Phi^{(1,3)}$, if any, can be arbitrary vectors in $\text{col}(U^{(1)})$.

We also use the similar idea to determine the column vectors of $\Phi^{(2,4)}$.

A.5. Training Details

Both our simulation in Sec. 5 and our evaluation in Sec. 6 run on a personal laptop with 2.7 GHz Intel Core i5 processor and 8-GB 1867 MHz DDR3 memory. Our code is based on Pytorch and the Adam optimizer is used. The number of samples (train/test), number of epochs, batch size, learning rate and corresponding runtime (for the whole experiment) are summarized in Table 2. Note that our simulation in Sec. 5 is based on synthetic data, so we only need a

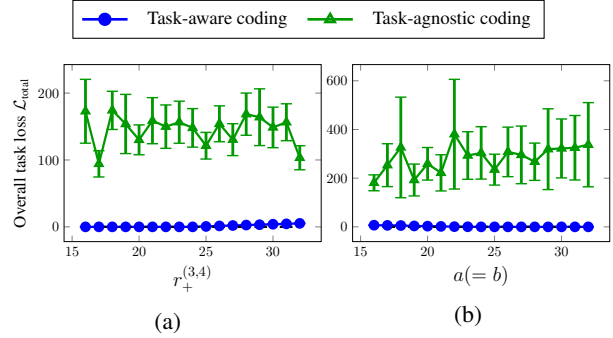


Figure 6. Simulation result with synthetic data of task-agnostic coding approach: overall task loss $\mathcal{L}_{\text{total}}$ under different $r_+^{(3,4)}$ (left) and different a (right).

training/testing dataset that satisfies $\mathbb{E}_x[x] = \mathbf{0}$, $\Psi = I$ and hence $2n = 64$ samples are enough.

Moreover, our evaluation in Sec. 6 also requires a pre-trained CNN classifier for 28×28 images, which is composed of two consecutive convolution layers and a final linear layer. The number of input channels, the number of output channels, kernel size, stride and padding for two convolution layers are 1, 16, 5, 1, 2 and 16, 32, 5, 1, 2 respectively, and ReLU activation and max pooling with kernel size 2 are used after each convolution layer. The final linear layer has input size 1568 and output size 1.

We also provide all our documented code as supplementary material and will make it publicly-available after the review process.

A.6. Overall Task Losses of Task-agnostic Coding Approach for Simulation

Fig. 6 shows the overall task losses of task-agnostic coding approach for the two simulation discussed in Sec. 5. For the purpose of comparison we also plot the overall task losses of our task-aware coding approach (same values as in Fig. 4). It clearly illustrates that task-agnostic coding approach performs more poorly than the task-aware coding approach.

A.7. Definitions of the Utilities in Evaluation

We first define the utility of $\phi^{(5,6)}$. We can find normalized vectors ξ_1, \dots, ξ_d that form an orthogonal basis of $\text{col}(\Phi^{(5,6)})$, where $d = \dim(\text{col}(\Phi^{(5,6)}))$. Then the utility of $\phi^{(5,6)}$ is defined as $\sum_{j=1}^d \xi_j^\top (S^{(3)} + S^{(4)}) \xi_j$, which is essentially the minimum achievable overall task loss difference between the case when node 3 and 4 receive nothing and when they receive $\phi^{(5,6)}$ only. For task-aware coding benchmark approach, according to A.4, the utility of $\phi^{(5,6)}$ equals the sum of the top- Z eigen-values of $S^{(3)} + S^{(4)}$.

We next define the utility of $\phi^{(1,3)}$. We can find nor-

Table 2. Training Details

Application	Num of Samples (Train/Test)	Num of Epochs	Batch Size	Learning Rate	Runtime
Simulation (Sec. 5)	64/64	2000	64	0.05	< 24 hrs
Evaluation (Sec. 6)	30000/5000	20	64	5×10^{-3}	< 48 hrs

(a) Original images.

(b) Reconstructed images, task-aware coding.

(c) Reconstructed images, task-aware no coding.

(d) Reconstructed images, task-agnostic coding.

(e) Reconstructed images, coding benchmark.

Figure 7. Original images and reconstructed images for different approaches ($Z = 10, \gamma = 0.9$). The first and the second row of each approach are the reconstructed images at node 3 and 4, respectively.

malized vectors χ_1, \dots, χ_e that extend ξ_1, \dots, ξ_d to an *orthogonal* basis of $\text{col}([\Phi^{(1,3)}, \Phi^{(5,6)}])$, where $e = \dim(\text{col}([\Phi^{(1,3)}, \Phi^{(5,6)}])) - d$. Then the utility of $\phi^{(1,3)}$ is defined as $\sum_{j=1}^e \chi_j^\top S^{(3)} \chi_j$, which is essentially the minimum achievable overall task loss difference between the case when node 3 receives $\phi^{(5,6)}$ only and when it receives both $\phi^{(1,3)}$ and $\phi^{(5,6)}$.

The utility of $\phi^{(2,4)}$ is defined similarly as $\phi^{(1,3)}$.

A.8. Comparison of the Reconstructed Images in Evaluation

In Fig. 7, we compare a few reconstructed images for different approaches in our evaluation (when $Z = 10, \gamma = 0.9$). For task-aware approaches, since the task loss of node 3 is

dominated by the reconstruction of the left feature map respectively, we see the left part of the reconstructed image at node 3 has a higher quality compared to the right part. And for node 4 we have similar observations. On the other hand, for task-agnostic coding approach, the quality difference between the left part and the right part is not as obvious as the task-aware approaches.